Uncertainty Propagation in Post-firing Analysis of SRM Internal Ballistics

F. Maggi, D. Viganò, and L. Galfetti

Politecnico di Milano, Aerospace Science and Technology Department
Space Propulsion Laboratory (SPLab)
I-20156, Milano, Italy

Abstract

Post-firing analysis of solid rocket motors enables the identification of important propulsion parameters such as characteristic velocity, discharge coefficient, throat erosion, burning time, and other details, depending on the degree of complexity involved in the analysis. Firing data can have different sources. Test-bench firings are usually carried on for evaluation purposes during design processes, prototype evaluation, or routine quality check in propellant production. Mission-related data may be obtained from in-flight streaming. In this respect, some types of information are not always available for in-flight tests. Throat erosion measurements are not accessible or the propulsion unit might not be fully instrumented, in case of production flights.

The accuracy featuring analysis results are influenced by both uncertainty of available data (e.g. random or systematic errors) and lack of knowledge for some parameters. The present work applies a methodology for uncertainty propagation to a simplified post-firing tool. The post-processing algorithm is based on a zero-dimensional framework capable of deriving characteristic velocity, thrust coefficient, throat erosion, and burning time. Code implementation and verification are presented. An example of uncertainty analysis is reported for a limited number of sources, both epistemic and aleatory. Propagation is traced using a Monte Carlo method and Latin hypercube sampling.

Nomenclature

Latin symbols

A_t	Throat area, m^2	$\dot{m}_t$	Throat mass flow rate, kg/s
A_b	Propellant burning area, m^2	N_{it}	Number of iterations
c^*	Characteristic velocity, m/s	P_e	Pressure at nozzle exit, Pa
c_F	Characteristic velocity, m/s	P_a	Ambient pressure, Pa
d_t	Throat diameter, m	r_b	Burning rate, mm/s
F	Thrust, N	t_0	Initial burning time, s
g_0	Standard gravity, m/s^2	t_b	End burning time, s
I_s	Specific impulse, s	u_e	Gas velocity at nozzle exit, m/s
M_p	Loaded propellant mass, kg	V_c	Combustion chamber free volume, m^3

Greek symbols

γ	Specific heat ratio	η_{cF}	Efficiency for c_F
Γ	Vanderkerkhove function	ρ_p	Propellant density, kg/m^3
η_{c^*}	Efficiency for c^*	ρ_c	Gas density, kg/m^3

Introduction

Thrust produced by a rocket motor depends on propellant mass flow rate, expansion properties and external pressure, and it is directly connected to combustion chamber characteristics. Performance deviations can be generated by intrinsic factors of the burning process, rocket production uncertainty, or external events connected to storage and use. These information are strictly connected to mission analysis. Estimation of delivered specific impulse or thrust-time history are of paramount importance since they partake in computation of mass budget and trajectory. Correlated coefficients (namely, thrust coefficient and characteristic velocity) represent useful engineering parameters that identify the behavior of nozzle and combustion chamber [1][2].

Among the potential propulsion systems, solid propellant missions can be very sensitive to performance variability. In launch applications the lack of commanded throttling impairs run-time mission corrections. A liquid-fueled platform should be implemented for compensation, within certain limits. Commanded de-orbiting using solid propulsion devices suffer from a double source of uncertainty: on one side, the rocket firing is affected by uncertainty, while on the other side mass and configuration of the apparatus in its end-of-life status is not well known. Atmospheric reentry, flight path angles and ground footprints may suffer from deviation of nominal behavior.

The real behavior of a rocket results from the overlapping of design performance and multiple undesired effects, spanning from production deviation, to performance detriment. Some of these factors can be predicted and are reproducible time after time. For example, most of specific impulse losses depend on reproducible events such as propellant agglomeration attitude, nozzle erosion, or chemical kinetics of expanding gases. Rather, loaded mass, grain dimensions, propellant bulk temperature at firing, very often are not predictable but are related to variability of production and operational environment. On this basis, statistical techniques can be used to rate the goodness of prediction and can supply a band of performance variability, supporting the analysis of success probability for a mission.

The analysis of post-firing data supply information about the real behavior of a propulsion unit, once operated in relevant environment or on a test-bench. Uncertainties derive from the quality of collected data but also from availability of accurate information about the experimented samples. The present paper describes a simple zero-dimensional model for post-firing analysis and performs uncertainty quantification on resulting propulsion parameters. Thrust and pressure traces are used to derive the evolution in time of mission-critical parameters, such as specific impulse, throat erosion, characteristic velocity, and thrust coefficient. In this presented version, internal ballistics is not addressed.

Post-firing analysis

When reconstructing from tests and operations, main observable parameters consist of pressure, measured in the combustion chamber, and thrust. Propulsion parameters and correlated coefficients can be derived after proper post-firing analysis. Thrust of solid rocket motors is generated by the expulsion from the nozzle of high-speed gases, plus a static contribution, if non-optimal expansion is considered. Equation (1) represents the general one-dimensional formulation.

$$F = \dot{m}_t u_e + (P_e - P_a) A_e \qquad \textbf{(1)}$$

where F is the thrust, $\dot{m}_t$ is the mass flow rate across the throat, P_e and A_e are respectively nozzle exit pressure and area, while P_a is ambient pressure. Main contribution to the mass flow rate exhausted from the nozzle is produced by propellant grain combustion but, in principle, other sources, such as ignition system and thermal protection degradation, supply further mass to the exhaust gases. The instantaneous performance can be summarized by Eq. (2) [3].

$$\frac{T}{g} = (\dot{m}_t I_s)_{prop} + (\dot{m}_t I_s)_{igniter} + (\dot{m}_t I_s)_{inerts} = (\dot{m}_t I_s)_{global} \qquad \textbf{(2)}$$

The propellant contribution is by far the most important. The igniter mass flow rate acts for a limited time during ignition transient, in the order of tens to few hundreds of milliseconds. Ablation rate of thermal protections is two or three orders of magnitude less than the propellant burning rate. Moreover, surface exposed to ablation is dependent on the peculiar grain design. Due to the simplicity of the proposed model, only propellant contribution is considered now.

The behavior of combustion chamber pressure results from the mass balance between discharged, produced, and accumulated combustion products. When a zero-dimensional modeling non-stationary mass conservation is represented by Eq. (3).

$$\frac{dp_c}{dt} = \frac{(\Gamma(\gamma)\, c^*)^2}{V_c}\left[(\rho_p - \rho_c)A_b r_b - \frac{p_c A_t}{c^*}\right] \quad \textbf{(3)}$$

This equation is implicitly assuming that the combustion chamber is featured by spatially uniform pressure and propellant burning rate. In general, rockets are equipped with head-end sensors to measure stagnation properties but total and static values of pressure may change along the grain due to non-isentropic processes and dynamic pressure effects, especially for propulsion units with large L/D (length-to-diameter) ratios. For most of small-scale test motors this condition is not present and the effect can be neglected. Rather, one-dimensional internal ballistic simulations should be implemented to correct the measured value from head- to aft-end.

If the analysis neglects ignition and tail-off transients, and rapid pressure variations are not present in the rocket, the assumption of quasi-steady behavior can be taken. In this case, the instantaneous relation between nozzle mass flow rate and internal pressure becomes $\dot{m}_p = p_c A_t / c^*$, where the characteristic velocity $c*$ is a thermochemical property of the combustion chamber. In a similar manner, thrust coefficient c_F correlates throat area A_t, pressure P_c and thrust with the formula $T = c_F P_c A_t$. Proper efficiencies $\eta_{cF} = (c_F)_{real}/(c_F)_{ideal}$ and $\eta_{c*} = (c^*)_{real}/(c^*)_{ideal}$ can be introduced to correlate ideal and real coefficients. Ideal data for c_F and c^* can be obtained either by analytical models or thermochemistry computational codes.

Simplified post-firing analysis

Model

The aim of the algorithm is the implementation of a simple post-firing analysis tool. The procedure used here is inspired to a similar algorithm proposed by Zhang and co-authors [4]. A zero-dimensional quasi-steady model is established for the computation of characteristic velocity, thrust coefficient, and instantaneous mass flow rate. The ideal value of $c*$ depends on specific heat ratio γ and on the flame temperature. Indirectly, the value depends on pressure. Tabulation of this parameter can be obtained either analytically from equilibrium combustion chamber data or by using a thermochemical code [5][6]. In this work NASA CEA software was adopted, interpolating the results using the power law reported in Eq. (4) .

$$c^*_{ideal} = c^*_{ref}\left(\frac{p_c}{p_{ref}}\right)^m \quad \textbf{(4)}$$

The ideal thrust coefficient can be derived analytically using Eq. (5) under the assumption of single-phase frozen combustion products, isentropic expansion, calorically perfect specific heat, and one-dimensional flow.

$$(c_F)_{ideal} = \sqrt{2\frac{\gamma^2}{\gamma-1}\left(\frac{2}{\gamma+1}\right)^{\frac{\gamma+1}{\gamma-1}}\left(1-\frac{p_e}{p_c}\right)^{\frac{\gamma+1}{\gamma}}} + \frac{p_e - p_a}{p_c}\frac{A_e}{A_t} \quad \textbf{(5)}$$

The use of an analytical expression for c_F, instead of a computed tabulation, simplifies the implementation since the parameter features a two-variable dependence (namely, external pressure and combustion chamber pressure), once

nozzle geometry and propellant formulation are fixed. If calorically perfect gas and frozen mixture assumptions are dropped, a tabulation based on thermochemical code should be implemented.

The computation of the efficiency parameter for the characteristic velocity, defined as the real-to-ideal ratio $\eta_{c^*} = (c^*)_{real} / (c^*)_{ideal}$, is based on Eq. (6). The formula integrates the instantaneous mass discharged from the nozzle and compares the result to the total propellant mass M_p.

$$\eta_{c^*} = \frac{\int_{t0}^{tb} \frac{p_c A_t}{c^*_{id}} dt}{M_p} \tag{6}$$

Initial and final burning times, respectively t_0 and t_b, must be identified from pressure traces. Several criteria exist in the open literature for the identification of relevant burning times in post-firing analysis of small scale rocket motors [7]. The current ballistic analysis identifies two instants when pressure during ignition and extinction crosses 1% of the maximum pressure. These definitions make the results sensitive to the shape of the pressure (e.g. long tail-off due to grain misalignment) but it was observed in past works that data scattering from post-firing analysis derives from intrinsic test variability and not from the specific adopted criterion [8].

For the computation of $\dot{m}_p$ an estimation of throat area evolution is necessary. The code should handle with the variation of throat area during firings, due to erosion or metal deposition. During steady rocket firings, the information can be retrieved by checking the diameter before and after the firing. If data are not available from post-firing measurements (as in post-mission analysis), reconstruction of nozzle behavior must be conducted from pressure and thrust, using the definition of c_F, as in Eq. (7).

$$A_t(t) = \frac{F}{\eta_{cF} \, (c_F)_{id} \; p_c} \tag{7}$$

A closed-loop analysis is set up to find a fitting law describing area increment in time. Efficiency of thrust coefficient is refined across iterations. It was observed from past researchers that the regression can be assumed linear for some extent, with the exception of transients and initial firing. In the latter case, throat restriction is observed, due to metal deposition [9]. In the present work, a simplified monotonic growth is assumed, enabling the computation of η_{c^*}. Efficiency of thrust coefficient is obtained by Eq. (8), in an inner loop of convergence. The formula stems from the definition of c_F and c^*, enforcing the equivalence of the combustion chamber pressure.

$$\eta_{cF} = \frac{F \;\; / (c_F)_{id}}{\dot{m} \; \eta_{c^*} \; (c^*)_{id}} \tag{8}$$

Verification

Code verification was performed using the pressure traces for a small-scale motor simulated by a ballistic code [10]. The motor is a 6.2 kg rocket with neutral pressure behavior [8]. Despite the original configuration is divergent-less, the present work considered a nozzle with expansion ratio of 4. The simulated propellant is an AP/Al/HTPB formulation (68/18/14 of mass fraction). The availability of a ballistic code enabled to test independently different aspects of the post-processing tool and to evaluate possible discrepancies. Throat erosion was simulated using a linear area increment. Rates causing a final increment of nozzle diameter $\boldsymbol{\Delta d_t}$ of 0, 1, 3, and 5% were tested. Pressure curves are reported in Figure 1.

Table 1. Identified and real throat erosion at the end of the firing.

Id.	Real Δd_t	Identified Δd_t
Bar00	0%	0.00%
Bar01	1%	1.00%
Bar03	3%	3.00%
Bar05	5%	5.03%

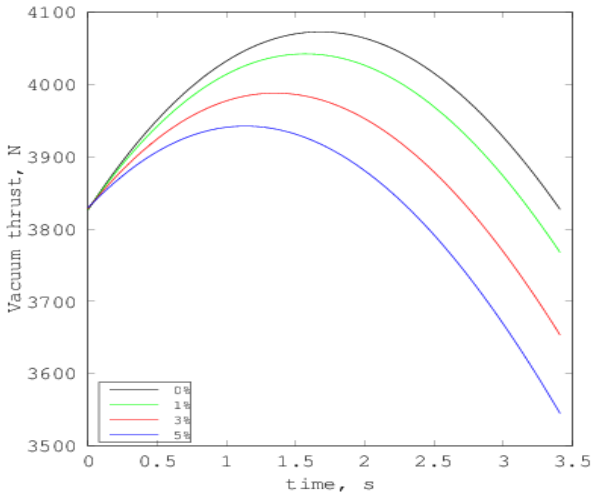

Figure 1. Simulated thrust data for BARIA rocket with divergent nozzle and parametric erosion of nozzle. Increment of throat radius is reported in the legend.

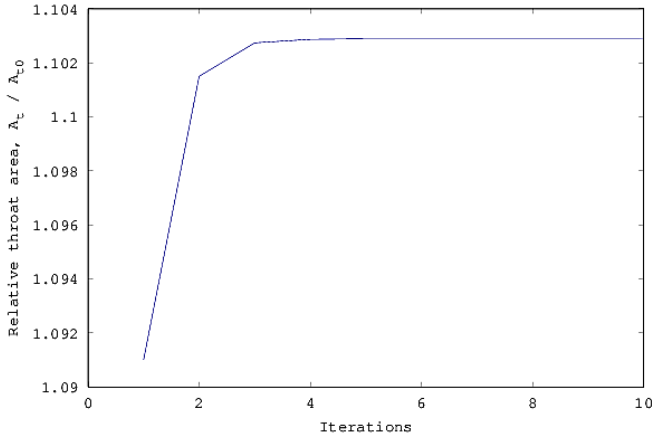

Figure 2 Iterations for detection of throat erosion.

Errore. L'origine riferimento non è stata trovata. reports the condensed results of identified final throat variation Errors between real and predicted data are less than 1%. The convergence path for a time step close to the burnout of the rocket is reported in Figure 2, showing that asymptotic behavior is visible after 5 iterations.

A comparison between mass flow rate (computed from ballistic model) and post-firing model is reported in Figure 3 and Figure 4. In this specific case, throat erosion was removed and operating pressure was about 7 MPa. The post-processing tool slightly overestimated the real instantaneous mass flow rate with an error of about 0.5%, constant across the firing..

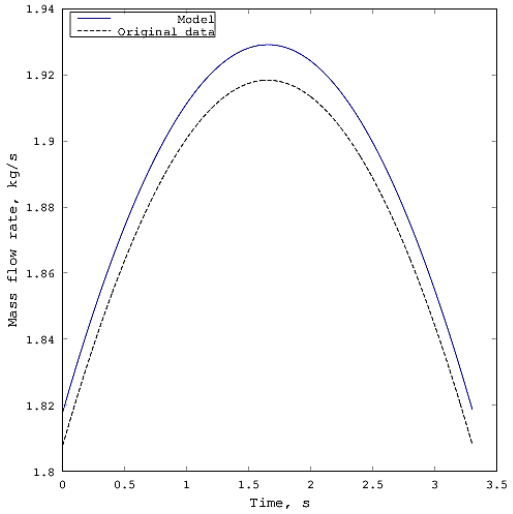

Figure 3. Comparison of identified mass flow rate with firing data.

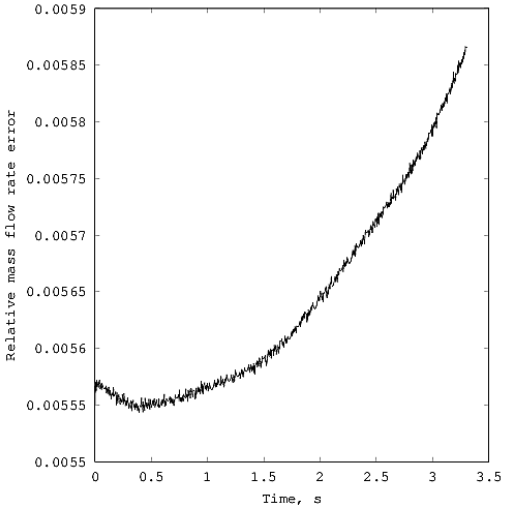

Figure 4. Relative error of mass flow rate identification.

Analysis of uncertainty

Statistic books and papers suggest Taylor Series (TSM) and Monte Carlo (MCM) methods for analysis of uncertainty propagation [11]. The technique connected to Taylor series is more analytic and requires the differentiation of model equations. The propagation of an uncertainty u for a generic two-equation variable $r = f(x, y)$ follows Eq. (9). In the formula, systematic standard uncertainty (b) and a random one (s) are mentioned. The correlation coefficient is zero if uncertainty sources are independent from each other.

$$u_r^2 = \left(\frac{\partial r}{\partial x}\right)^2 b_x^2 + \left(\frac{\partial r}{\partial y}\right)^2 b_y^2 + \left(\frac{\partial r}{\partial x}\right)^2 s_x^2 + \left(\frac{\partial r}{\partial y}\right)^2 s_y^2 + (correlation\ effect) \quad \textbf{(9)}$$

The MCM methodology consists in running several instances of a model, introducing uncertainty by randomly sampling data from appropriate probability distributions. The method can be quite simple to implement but requires a consistent computational power for convergence, when multivariate problem is solved. The simplicity and generality of the MCM makes it very suitable for uncertainty propagation analysis in presence of complex problems, where analytical description is not possible or complex. This second option is chosen in the present paper.

Uncertainty sources must be identified for proper representation in MCM. The task is not easy, especially if the full knowledge of the modelled system is not available. In this respect, the framework proposed by Oberkampf can be useful [12][13]. In addition to the classification of systematic and random error, the sources of uncertainty can be

grouped as *aleatory* or *epistemic*. The *aleatory* uncertainty derives from the intrinsic variability of a process. This kind of source can be included when a sufficient knowledge of the event is achieved and a probability distribution function can be inferred for its representation. The *epistemic* uncertainty is represented by those sources of error that do not derive from natural fluctuation of variables but stem from the lack of knowledge of the tested system. Missing specifications, lack of experimentation, and other similar sources are typical examples. The bounds of these uncertainties can be reduced if a better knowledge is obtained. The treatment of these two families of sources should be segregated, according to Oberkampf. In the case where a model or a project is commenced, or knowledge from the system is fully missing, all uncertainties should be treated as epistemic and their propagation can be dealt together. As the knowledge of the system under consideration is extended, part of data become available and fractions of epistemic uncertainty becomes aleatory, changing the probability distribution according to the accumulated knowledge-base. A variable is *deterministic* if its value is known a-priori (such as constants) or its uncertainty can be neglected in relation to the effect on propagation.

The MCM requires that each variable is probed according to a well-defined probability density function. Type and width depend on the knowledge of the problem. A Normal distribution is good representation for aleatory sources. In this case, standard deviation is available existing data or prior tests. In some cases, missing information or limited knowledge of the system do not enable the assumption of a specific data distribution, of an averaged value, or of a standard deviation. However, it is possible to acquire the notion of the expected parameter range. Uniform probability density functions are good representations of these latter types. Case by case considerations should verify which condition better applies. This approach enables the inclusion also of errors found in sub-model validation, in curve integration or numerical representation, and in other verified sources, if a proper metrics can be defined [13].

The representation of results and the identification of final confidence interval for cases where both aleatory and epistemic uncertainties are present cannot follow the usual statistical procedures. The use of a *six-sigma* criterion implicitly assumes that results can be approximated by a probability density function. This is not the case when epistemic input data are present. A better description consists in using a *p-box* (probability box) representation and an interval of confidence that is based on it. The *p-box* is a plot for cumulative probability distribution, containing a bounding interval where the results will be found. The interpretation of a p-box gives a direct representation of uncertainty bounds for different levels of confidence.

Uncertainty propagation

Identification and propagation of uncertainty sources towards global performance parameters are considered for the aforementioned simplified post-processing tool. At this stage, variability of mean data values across different firings is considered, while scattering within the single test (e.g. pressure oscillations) is neglected because it does not influence output parameters. List of sources can be derived by considering the formulas of Eq. (6) and (8). Current analysis will be limited to thrust, combustion chamber pressure at the nozzle side, loaded propellant mass, burning time, and thermodynamic properties. The list can be easily extended following the same conceptual framework.

The instantaneous thrust is a project specification for a rocket motor with a stated bound of confidence around a nominal value. This is an aleatory variable because the knowledge of the system allows to expect that the delivered thrust will be located within known confidence bounds. A Normal probability distribution is assumed for the population. A parametric investigation on error bounds of 1, 3, and 5% is considered. For simplicity, the same trend is used for variability of the head-end pressure. Another aleatory variable consists of the propellant loaded in the rocket. The nominal value is known but random variability due to production process can be present. A normal distribution with 1% error is assumed. If reconstructing from flight data, error in altitude evaluation due to trajectory reconstruction will propagate on ambient pressure. A normal distribution with 3% error bound is assumed.

Aft-end total pressure depends on losses across the rocket. The parameter is not known a-priori and a parametric analysis is done on three different classes of decrements (0, 1.5, and 3%). The thermodynamic parameter c^* should be treated as deterministic, if design and analysis tool are based on the same data set. This is not true if original data are not available. In the presented case, original thermodynamic data are not available. It was observed that data may

differ between different thermochemical codes and the analytical formulation of c^*. Due to lack of knowledge, the variability is catalogued as epistemic, assuming a 4% bound of uniform variability.

A series of preliminary MC analyses have been performed on a restricted data set to set up the number of iterations. In order to reduce the amount of runs before convergence, Latin Hypercube sampling was applied, using 500 and 1000 samples and looking at the standard deviation of η_{c^*} for the firing and of $\dot{m}_p$ and of η_{cF} at half of combustion time.

Table 2. Convergence tests for MC simulations.

	$N_{it} = 500$	$N_{it} = 1000$
$\sigma_{\dot{m}}$ at t = 1.5 s	0.0064	0.0065
$\sigma_{\eta_{cF}}$ at t = 1.5 s	0.0099	0.0098
$\sigma_{\eta_{c^*}}$	0.0103	0.0106

The input confidence interval was set to 3% for thrust and altitude. Head-to-aft end pressure loss was set to 1.5% and ideal C* was computed by CEA code. Results of Table 2 shows suggest that the aleatory component for this MC method with 500 sampling iterations is converged.

Results

Monitored variables consist of mass flow rate and efficiency of thrust coefficient at half of combustion time, and efficiency of characteristic velocity. Results are reported in a series of P-boxes collecting data for similar variability of thrust. Partial representations showing only some selected curves are reported in Figure 5 for thrust confidence level of 1%. Condensed results are reported from Table 3 to

Table **6**. Reference percentiles 0.1, 0.5, and 0.9 identify the values that upper-bound the 10%, 50%, and 90% of the result population. Each value is not identified by a number but by intervals, generated by the compresence of aleatory and epistemic data. The larger is the interval, the larger is the range where the interested value might fall. The overall set of cumulative curves can identify minimum and maximum values for these data. The narrower is the interval, the better is the identification of the distribution. The reader should note that these intervals are generated by epistemic uncertainties and, thus, by unknown aspects of the problem. Better knowledge would tighten the variability, letting better identification of variability due to aleatory causes.

From the comparison of data it appears that mass flow rate identification features a limited sensitivity on any kind of uncertainty. The location of the median (cumulative distribution 0.5) is always within an interval spanning less than 1%, regardless of the different uncertainty sources. Also expected data range is not wider than about 1%. This fact suggests that there is good reliability for mass flow rate identification from the present algorithm.

The parameter η_{c^*} is an average value for the whole firing. Its variability depends upon both ideal c^* knowledge and aleatory variation of the thrust. Non-physical results are obtained for increased uncertainties. Identification in this case is not precise and the range of variation can exceed 10%, in some cases. The reduction of ideal c^* uncertainty to 2% removes the problem of unphysical data but interval of identification is still high. For example, the median can be located with a variability of 7%.

The parameter η_{cF} follows the trend of thrust variability. Expected range becomes wider as confidence interval of thrust is incremented from 1% to 5%, passing respectively from 7% to 14%. For the condition of 5% of uncertainty on thrust, the identification of the median and of the percentile at 0.9 are not altered while the percentile at 0.1 becomes wider, highlighting that particularly disadvantageous conditions can be generated.

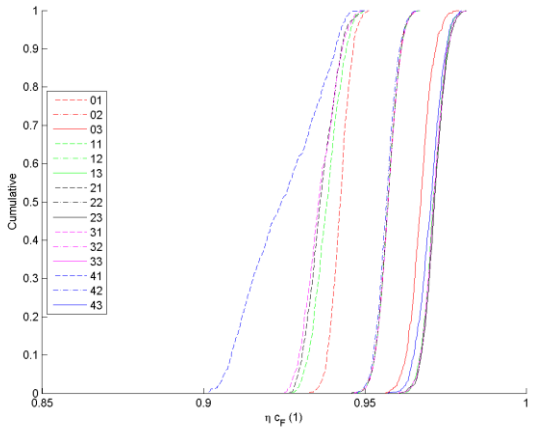

a) η_{cF}

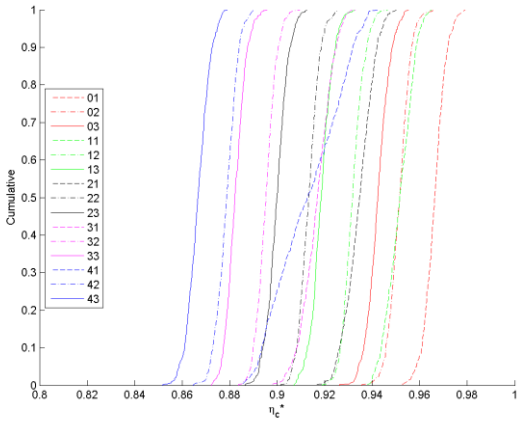

b) η_{c^*}

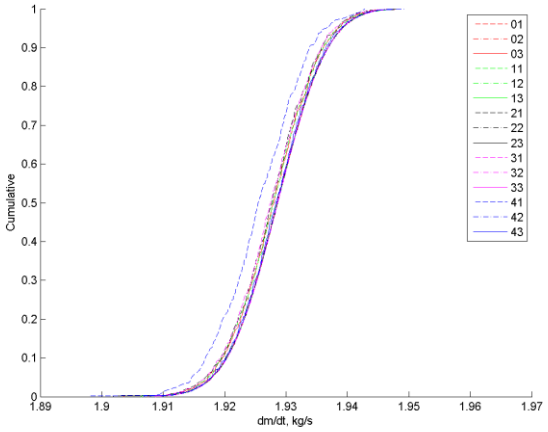

c) $\dot{m}_p$

Figure 5. Examples of p-boxes generated by cumulative distributions (only representative distributions are reported). Thrust confidence interval: 1%.

Table 3. Intervals of relevant points for cumulative distributions. Thrust confidence interval: 1%.

Cumulative	**0.1**	**0.5**	**0.9**
$\dot{m}$	1.9168 – 1.9204	1.9255 – 1.9287	1.9338 – 1.9369
η_{c^*}	0.8610 – 0.9609	0.8666 – 0.9663	0.8726 – 0.9717
η_{CF}	0.9086 – 0.9674	0.9240 – 0.9715	0.9408 – 0.9758

Table 4. Intervals of relevant points for cumulative distributions.
Thrust confidence interval: 3%. Unphysical results are marked with a star (*).

Cumulative	0.1	0.5	0.9
$\dot{m}$	1.9162 – 1.9204	1.9253 – 1.9286	1.9334 – 1.9368
η_{c*}	0.8544 – 0.9582	0.8659 – 0.9806	0.8771 – 1.003(*)
η_{CF}	0.9143 – 0.9593	0.9331 – 0.9717	0.9498 – 0.9845

Table 5. Intervals of relevant points for cumulative distributions.
Thrust confidence interval: 3%. Reduced uncertainty on c^*: 2%.

Cumulative	0.1	0.5	0.9
$\dot{m}$	1.9162 – 1.9204	1.9257 – 1.9286	1.9342 – 1.9368
η_{c*}	0.8696 – 0.9387	0.8823 – 0.9548	0.8936 – 0.9740
η_{CF}	0.9183 – 0.9593	0.9357 – 0.9717	0.9498 – 0.9845

Table 6. Intervals of relevant points for cumulative distributions.
Thrust confidence interval: 5%. Unphysical results are marked with a star (*).

Cumulative	0.1	0.5	0.9
$\dot{m}$	1.9110 – 1.9202	1.9210 – 1.9285	1.9319 – 1.9368
η_{c*}	0.8497 – 0.9592	0.8702 – 1.014(*)	0.8896 – 1.061(*)
η_{CF}	0.8596 – 0.9513	0.9077 – 0.9717	0.9492 – 0.9929

Final considerations

A Monte Carlo analysis has been performed to assess uncertainty propagation in a simple post-firing analysis tool. The methodology grounded on the identification of epistemic and aleatory variables. Segregated treatment of these classes of variables enabled the identification of bounds of uncertainty which derive from the lack of knowledge of the input parameters to the model. The final result consisted in the identification of a *p-box*, which bounds give information on results reliability.

Regarding the post-processing tool, it appears that the algorithm features good accuracy and good precision for the identification of the mass flow rate in different conditions. The precise knowledge of the loaded propellant mass is a prerequisite. Other sources of uncertainty do not propagate in this result. Confidence level for efficiencies are quite high when ideal parameters are not known and when error on real thrust increases. The former parameter derives from the design knowledge-base and can be improved if data are released. The latter input depends on parent

algorithm, and on sub-models for rocket drag identification and on integral of discharged mass flow rate. The characterization was performed on data obtained from a simulated small scale rocket motor.

Acknowledgement

The present work was developed in the frame of the MVFLAU project, ESA contract No. 4000108350/13/NL/MH.

References

[1] J.P. Sutton and O. Biblarz. Rocket Propulsion Elements, Seventh Edition, Wiley, 2001.
[2] W.H. Heiser and D.T. Pratt. Hypersonic Airbreathing Propulsion, AIAA Educational Series, AIAA, Washington, DC, USA, 1994.
[3] Anon., Solid Rocket Motor Performance Analysis and Prediction, SP-8039, NASA, 1971.
[4] W. Zhang et al. “Identification of throat radius variation for solid rocket motor”. AIAA Paper 1997-2724.
[5] S. Gordon and B.J. McBride. “Computer program for calculation of complex chemical equilibrium compositions and applications”. NASA Reference Publication RP-1311, 1996.
[6] I. Glassman and R.F. Sawyer. “The performance of chemical propellants”. AGARDograph 129, AGARD, France, 1970.
[7] R.S. Fry, Evaluation of Methods for Solid Propellant Burning Rate Measurements, NATO/RTO Advisory Report, AVT Working Group 16, 2002.
[8] F. Maggi, et al. "Burn-rate measurement on small-scale rocket motors". Defence Science Journal 56.3 (2006): 353-367.
[9] A. Annovazzi. Private communications, Dec. 2014.
[10] D. Viganò, F. Maggi, and A. Annovazzi. “Monte Carlo Method for Uncertainties Quantification of SRM Internal Ballistics Model”. 11th PEGASUS-AIAA Student Conference, Salon de Provence, France, 2015.
[11] H.W. Coleman and W.G. Steele. Experimentation, Validation, and Uncertainty Analysis for Engineers, Third Edition, Wiley, 2009.
[12] W.L. Oberkampf, et al. "Error and uncertainty in modeling and simulation". Reliability Engineering & System Safety 75.3 (2002): 333-357.
[13] C.J. Roy and W.L. Oberkampf. “A comprehensive framework for verification, validation, and uncertainty quantification in scientific computing”. Computer Methods in Applied Mechanics and Engineering 200.25 (2011): 2131-2144.